Electric field driven molecular recognition reactions of Guanine with 1,2-dipalmitoyl-*sn*-glycero-3-cytidine monolayer deposited on Gold Electrodes

Julia Alvarez-Malmagro[a,b], ZhangFei Su[b], J. Jay Leitch[b], Francisco Prieto[a *], Manuela Rueda[a *], Jacek Lipkowski[b *]

[a]Department of Physical Chemistry, University of Seville, C/Profesor García González n◦ 2, 41012 Seville, Spain.

[b]Department of Chemistry, University of Guelph, Guelph, Ontario, Canada N1G 2W1.

Corresponding authors:

Francisco Prieto: dapena@us.es

Manuela Rueda: marueda@us.es

Jacek Lipkowski:jlipkows@uoguelph.ca

Abstract

Monolayers of 1,2-dipalmitoyl-*sn*-glycero-3-cytidine were incubated with guanine in a 0.1 M NaF electrolyte at the surface of a Langmuir trough and transferred to gold (111) electrodes using the Langmur-Schaefer (LS) technique. Chronocoulometry and photon polarization modulation infrared reflection absorption spectroscopy (PM-IRRAS) were employed to investigate the influence of the static electric field on the orientation and conformation of the nucleolipid molecules on the metal surface and to monitor the molecular recognition of guanine with the cytosine moiety of the nucleolipid When the monolayer is exposed to guanine solutions, the cytosine moiety binds to the guanine residue in either a Watson-Crick complex at

positively charged electrode surfaces or a non-complexed state at negative surface charges. The positive electrostatic field causes the cytosine moiety and cytosine-guanine complex to adopt an early parallel orientation with respect to the plane of the monolayer with a measured tilt angle of ~10^{o}. The parallel orientation is stabilized by the interactions between the permanent dipole of the cytosine moiety or Watson Crick complex and the static electric field. At negative charge densities, the tilt of the cytosine moiety increases by ~15^{o} ─20^{o} destabilizing the complex. Our results demonstrate that the static electric field has an influence on the molecular recognition reactions between nucleoside base pairs at the metal-solution interface and can be controlled by altering the surface charge at the metal.

1. Introduction

Host–guest interactions occurring at the surface of an electrode surface modified with a functional monolayer constitute the basis for the development of molecular sensors. Over the past several years, we have investigated molecular recognition reactions between complementary nucleic acid base pairs in monolayers adsorbed at the gold-solution interface.[1–6] However, when the bases are directly adsorbed at the gold electrode surface, the gold-base interactions have competed with the base-base interactions. Independently, several studies on nucleolipid monolayers spread at the air-solution interface demonstrated that these systems are attractive for investigating molecular recognition reactions between complementary bases of nucleic acids.[7–13] Using the knowledge gained from these previous studies, we recently assembled a monolayer of 1,2-dipalmitoyl-*sn*-glycero-3-cytidine (Figure 1) at the gold electrode surface where the cytidine moiety was directed to the solution and separated from the metal by the long hydrocarbon lipid chains.[14] With the help of photon polarization modulation IR absorption spectroscopy (PM-IRRAS), we have demonstrated that the static electric field affects the orientation of the polar head region controlling the tilt and rotation of the cytosine moiety with respect to the surface normal.[14]

The objective of the present study is to use this information to investigate the effect of the electric field on the cytosine-guanine molecular recognition reaction. Cytosine and guanine

are complementary nucleic acid bases involved in the formation of the DNA double helix.[15] We will show that guanine binds to the monolayer of 1,2-dipalmitoyl-*sn*-glycero-3-cytidine assembled at the gold (111) surface and that the applied electrode potential has a significant impact on whether guanine forms a complex with the cytosine moiety or inserts into the film through non-specific interactions. This study provides unique molecular level information how the static electric field can be used to promote nucleoside recognition reactions. This information is significant for future biosensor development.

a) Guanine (G)

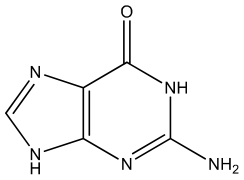

b) 1,2-dipalmitoyl-sn-glycero-3-cytidine nucleolipid

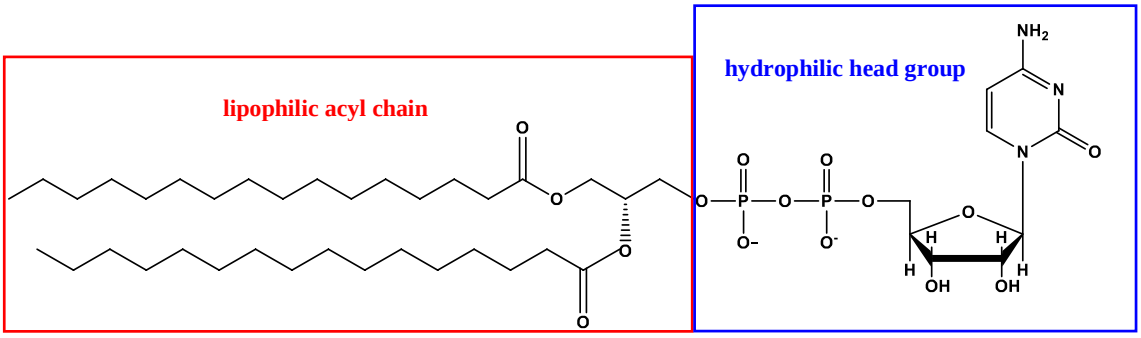

Figure 1. a) Molecular structure of guanine, b) structure of 1,2-dipalmitoyl-sn-glycero-3-cytidine diphosphate nucleolipid. diphosphate

2. Experimental.

The experimental procedures and data analysis were described in the preceding paper.[14] However, for completeness, we are reproducing the most significant aspects and information.

2.1. Reagents, solutions, electrodes and materials.

1,2-dipalmitoyl-sn-glycero-3-cytidine diphosphate (Avanti Polar Lipids) was dissolved in chloroform at a concentration of 1 mg mL^{-1} and used as the stock solution for spreading nucleolipid monolayers at the Langmuir trough surface. The sodium fluoride powder (BioXtra, 99%, Sigma-Aldrich) was cleaned in an UV ozone chamber (UVO cleaner, Jelight, Irvine, CA) for 15 minutes to oxidize organic impurities. Cytosine, guanine, guanosine-5'-diphosphate were purchased from Sigma Aldrich and used without additional purification. The NaF supporting electrolyte (0.1 M) was prepared by dissolving the cleaned NaF powder in ultrapure water (resistivity > 18.2 MΩ cm), procured from a Milli-Q UV plus water system (Millipore, Bedford, MA).electrolyte. D_2O (Cambridge Isotope Laboratories, Cambridge, MA) was used as the solvent in the transmission and PM-IRRAS experiments.

Gold (111) electrodes were used as working electrodes in the electrochemical and PM-IRRAS experiments. Before each experiment, the single crystal face of the gold (111) electrode was cleaned twice by flame-annealing and cooling in air. In electrochemical experiments, a flame-annealed gold coil and Ag/AgCl electrode (saturated KCl), (Pine Research Instrumentation, Durham, NC) were used as a counter and reference electrode, respectively. In the PM-IRRAS measurements, a Pt foil and Ag/AgCl (saturated KCl) electrode were used as a counter and reference electrode, respectively. All experiments were performed at room temperature (20 ± 2 °C) and the potentials are reported versus the saturated calomel electrode (SCE) where the potential difference between SCE and Ag/AgCl was −0.045 V.

All glassware, including the electrochemical cell, was cleaned either in a potassium permanganate bath overnight or in a 3:1 v/v hot acid mixture of concentrated sulfuric: nitric acid for 2 h. The glassware was then thoroughly rinsed with Milli-Q water. All Teflon parts were cleaned in piranha solution ($3H_2SO_4$: $1H_2O_2$) and rinsed with copious amounts of Milli-Q water.

2.2. LB trough: pressure-area isotherms and sample preparation.

Surface pressure-area isotherms of 1,2-dipalmitoyl-*sn*-glycero-3-cytidine diphosphate in the presence of guanine were recorded at the air-solution interface using a Langmuir through (KSV NIMA, Biolin Scientific, Gothenburg, SE) equipped with two hydrophilic barriers and a Wilhelmy plate (surface area is 243 cm^2) made from filter paper. KSV LB5000 software was used to control the trough and to measure the isotherms. The subphase for the isotherm measurement was 0.1 M NaF aqueous solution with 0.025 mM guanine. The subphase was heated to temperature of 44 ± 1 °C, then the 1,2-dipalmitoyl-*sn*-glycero-3-cytidine stock solution in chloroform was spread onto the subphase surface. After 15 minutes allowed for solvent evaporation, the compression isotherms were recorded. About 20 min was allowed for the monolayer to be exposed to guanine in the subphase.

For the electrochemical and PM-IRRAS measurements, the 1,2-dipalmitoyl-*sn*-glycero-3-cytidine diphosphate monolayer was transferred to the gold (111) electrode at a surface pressure of 30 mN/m using the Langmuir-Schaefer (LS) method. The monolayer was compressed to 30 mN/m and then 10-15 min was allowed for guanine to attach to the head group of the nucleolipid. In the absence of guanine good reproducibility was observed for the compression and decompression cycle. In the presence of guanine no decompression measurements were performed to avoid intercalation of guanine between the acyl chains of the nucleolipid. The monolayer was dried at the surface of the gold (111) for 1 h prior to further experimentation. The LS method ensures that nucleolipid molecules are oriented with the cytosine moiety towards the bulk solution at the gold-electrolyte interface. The monolayer transferred to the gold (111) surface should adopt the same packing density as the monolayer formed at the air-solution interface.

2.3. Electrochemical instrumentation and measurements.

Electrochemical measurements were performed using potentiostat /galvanostat (HEKA PG590) and a lock-in amplifier (EG & G Instruments 7265 DSP). All data was collected using a

plug-in acquisition card (NI PCI-6052E) and custom-made software. The electrochemical measurements were carried out in an all-glass three-electrode cell. Contact between gold (111) working electrode and the supporting electrolyte was made using hanging meniscus configuration. The cell was purged with argon for 30 minutes prior to each experiment and a blanket of argon was maintained above the supporting electrolyte throughout the duration of the experiment. The electrolyte purity was checked by recording differential capacitance curves in the electrolyte solution and comparing with a reference result described previously.[16,17] The surface charge densities at the gold (111) electrode were measured using chronocoulometry.[16,18,19] The charge densities for the monolayer-covered electrodes were performed using the following series of potential steps: 1) base (E_b) potential was held at E = −0.20 V vs SCE for a period of 60 s and then stepped to final potential (E_f) for a period of 200 ms. The charge difference between E_b and E_f was measured by integration of the charging current curves. The potential was then returned to E_b for another waiting time of 60 s and was then stepped again to E_f where the value was changed from −0.15 V to 0.4 V vs SCE in 50 mV increments. 2) A similar sequence of potential steps was applied from E_b = −0.20 V vs SCE to E_f where the value was changed from −0.25 V to −0.4 V vs SCE. 3) Finally, a train of potential pulses was applied from E_b variable from −0.4 V to −0.85 V vs SCE to a constant final potential of −0.9 V vs SCE where total desorption of the monolayer takes place at the electrode surface. This program of potential pulses ensured a minimum perturbation of the monolayer structure by reducing to minimum potential steps to desorption of the monolayer. For the supporting electrolyte, the charge density curve was determined by stepping from a variable E_b to a constant E_f = −0.9 V vs SCE, waiting 60 s at E_b between each consecutive potential step using 0.05 V intervals. The potential of zero charge for the supporting electrolyte was determined independently from the position of the diffuse layer minimum of the capacitance in diluted electrolytes.[17,18] This value was used to convert the charge difference values into the absolute charge densities. For the electrode covered by the monolayer, the absolute charge

densities were determined by merging the charge difference curve with the curve for the supporting electrolyte at potential −0.8 V vs SCE where a total desorption of the monolayer was observed.[18,19]

2.4. Spectra collection and processing.

2.4.1. Transmission spectra and sample preparation.

Transmission spectra of 10 mM cytosine (Sigma Aldrich) in D_2O, 3.34 mg/ml guanosine 5 diphosphate (Sigma Aldrich) in D_2O and a mixture of 5 mM cytidine 5-diphosphate and 5 mM Guanosine 5-diphosphate in a 0.1 M NaF/D_2O electrolyte were measured using a home-made Teflon cell equipped with two circular CaF_2 windows separated by 50 μm Teflon spacer. A total of 1000 scans were collected using a resolution of 4 cm^{-1}.

2.4.2. PM-IRRAS spectra.

PM-IRRAS measurements were carried out with a Nexus 870 FT-IR spectrometer (Madison, WI) equipped with an external tabletop optical mount (TOM), MCT-A detector, photoelastic modulator (Hinds Instruments PM-90 with a II/ZS50 ZnSe 50 kHz optical head, Hillsboro, OR) and a sampling demodulator (GWC Instruments Synchronous Sampling Demodulator, Madison, WI). An electrochemical cell fit with a 1 in. CaF_2 equilateral prism (Boxin Photoelectric Co.) was used in the IR measurements. The prism was cleaned with water and methanol and then placed in the UV-ozone cleaner for 10 minutes prior to assembly of the IR cell. The TOM box was purged with a dry, CO_2-free air, which was provided by a purge gas generator (Parker Balston, Haverhill, MA) for ~5 h prior to and during the experiment. The electrode was pressed against the IR window to create the thin film configuration. The electrolyte thickness was ~4 μm, which was calculated as previously described.[20] The applied electrode potential was scanned from 0.34 V to −0.75 V vs SCE with steps of 0.1 V. In-house software, an Omnic macro, and a digital-to-analog converter (Omega, Stamford, CT) were used

to control the potentiostat (EG&G PAR362, Princeton, NJ) and collect a total of 4000 scans with a resolution of 4 cm^{-1}, which were averaged at each potential. The measurements were performed with a photoelastic modulator (PEM) set to half-wave retardation of 1600 cm^{-1} with an angle of incidence of 60° for the IR region pertaining to the head group. For the CH stretching region of the acyl chains, the half-wave retardation was set to 2900 cm^{-1} and the angle of incidence to 56°. These values were selected to obtain a large enhancement of the mean square electric field strength (MSEFS) of *p*-polarized radiation at the electrode surface.[14]

After correction for the photoelastic modulator (PEM) response functions,[21] the PM-IRRAS spectra were plotted in terms of ΔS , which is proportional to the absorbance of molecules adsorbed on the electrode surface and defined as:

$$\Delta \square = \frac{2(\square_{\square} - \square_{\square})}{\square_{\square} + \square_{\square}} = 2.3 \square \Gamma_{\square} \qquad (1)$$

where I_s and I_p are the intensities of the *s*- and *p*-polarized radiation, $\Gamma_{\square}$ is the surface concentration of the adsorbed species and $\square$ is the decadic molar absorption coefficient of the adsorbed species. The details of the PM-IRRAS measurement and data processing were described previously.[21]

2.4.3. Simulation of the PM-IRRAS spectra of the monolayer.

A homogeneous parallel phases system (gold/nucleolipid film/D_2O/CaF_2) was used as a model to simulate PM-IRRAS spectrum of randomly oriented 1,2-dipalmitoyl-*sn*-glycero-3-cytidine monolayer using in-house software that solves Fresnel equations by employing the transfer matrix method.[20] The thickness of the 1,2-dipalmitoyl-*sn*-glycero-3-cytidine monolayer was assumed to be equal to 3 nm, which is a half of the thickness of DPPC bilayer.[22] The optical constants of gold, D_2O and CaF_2 were taken from literature.[23,24] The optical constants were

calculated from the transmission spectrum of 1,2-dipalmitoyl-*sn*-glycero-3-cytidine diphosphate.

The directions of the transition dipoles for vibrations of the cytosine moiety of the nucleolipid were determined from DFT calculations of vibrational spectra for cytidine. The hybrid functional PBE[25] and 6-311++G(d,p) basis set present in the Gaussian 09 package were used in these calculations.[26] The effect of the solvent on the isolated molecule was treated by the continuum polarization model (PCM).

3. Results and discussion.

3.1. Compression isotherm studies.

Figure 2 shows the compression isotherms for the monolayer of 1,2-dipalmitoyl-sn-glycero-3-cytidine spread on the 0.1 M NaF subphase without and with 0.025 mM guanine. The presence of guanine in the subphase has a small effect on the compression isotherm. However, there are significant differences between compression isotherms measured on pure water and on 0.1 M NaF as the subphase. The inset to Figure 2 shows the compression modulus defined as:[8]

$$C_s^{-1} = -A\left(\frac{\partial \pi}{\partial A}\right)_T \qquad (2)$$

where A is the area per molecule and π is the surface pressure of the monolayer. For monolayers spread on the 0.1 M NaF, the C_s^{-1} values are lower than 80 mN m^{-1} in the entire range of surface pressures. These numbers suggest that the monolayers are predominantly in the liquid-expanded

state (LE). For the monolayer spread on the pure water subphase, the compression modulus increases rapidly at surface pressures greater than 30 mN m^{-1}, indicating a transition from the liquid-expanded to the liquid-crystalline state. The phase transition manifests as a minimum on the compression modulus curves, which is observed at ~30 mN m^{-1} (black curve) for the system using a pure water subphase. This minimum is significantly shifted to a value of ~50 mN m^{-1} for

nucleolipid monolayers spread on the surface of the 0.1 M NaF aqueous subphase. The presence

of electrolytes in the subphase has significant impact on the properties of the monolayer. Similar strong effect of the electrolyte on aggregation of cytidine nucleolipids was observed by Alies et al.[27] All three films merge at a collapse pressure of ~70 mN m^{-1} suggesting that the maximum packing density of the cytidine nucleolipid is ~52 A^2. It should be noted that the collapse pressure of pure DPPC monolayers on water is ~60 mN m^{-1} with a packing density of ~42 $Å^2$,[28] therefore, the values obtained for the cytidine nucleolipid are reasonable since the head group of the cytidine nucleolipid is larger than DPPC and carries an overall negative charge. For further analysis, the monolayers were transferred from the air-solution to the gold electrode surface at the film pressure of 30 mN m^{-1}, which corresponds to the mean molecular area equal to 102 A^2 and surface concentration, Γ, of 1.62×10^{-10} mol cm^{-2}.

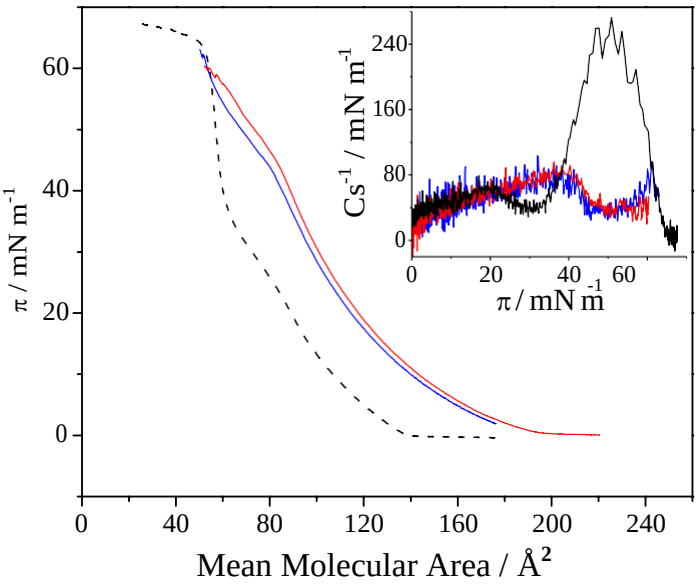

Figure 2. π-A isotherms of the 1,2-dipalmitoyl-*sn*-glycero-3-cytidine monolayers on the on the aqueous 0.1 M NaF subphase at 44 ºC in the absence (blue) and presence (red) of 25 µM guanine. The dashed line represents the compression isotherm of the 1,2-dipalmitoyl-*sn*-glycero-3-cytidine monolayer on a pure water subphase surface.The inset shows a plot of the compression modulus for the monolayers with (red curve) and without guanine (blue curve) on the 0.1 M NaF subphase compared with the compression modulus for the nucleolipid monolayer on a pure water subphase (black) in the absence of guanine.

3.2. Electrochemical measurements.

Figure 3 shows charge density curves for 1,2-dipalmitoyl-*sn*-glycero-3-cytidine monolayers deposited onto the gold (111) electrode from the 0.1 M NaF subphase in the absence (blue triangles) and presence of guanine (red circles). The charge density curve for the monolayer with guanine is somewhat lower than the curve of the monolayer without guanine. The potential of zero charge for the monolayers exposed to guanine amounts to −0.24 ± 0.04 V vs SCE. The potential of zero charge is influenced by the adsorption of anions and depends on orientation of surface dipoles.[29] Since the surface concentration of lipids is known, the charge densities could be used to calculate the electrosorption valency and charge number on the lipid using the procedure described in.[19,30–32]

The electrosorption valency and charge number calculations are described in section 1 of the Supporting Information and the calculated electrosorption valencies and charge per adsorbed molecule are plotted in Figures S1 and S2, respectively. Within the experimental uncertainty, the charge number on the monolayers in the absence and presence of guanine has values of ~1.3 and show no potential dependence from +0.3 to −0.3 V vs SCE. Since 1, 2-dipalmitoyl-*sn*-glycero-3-cytidine diphosphate is dianionic, the value of 1.3 indicates that counter ions are present in the head group region of the monolayer to screen the charge of the diphosphates. At potentials more negative than −0.4 V vs SCE, the charge density curves for electrodes covered by the monolayers merge with the curve of the supporting electrolyte at −0.8 V vs SCE, which indicates electrodewetting of the organic film from the electrode surface.[33–35]

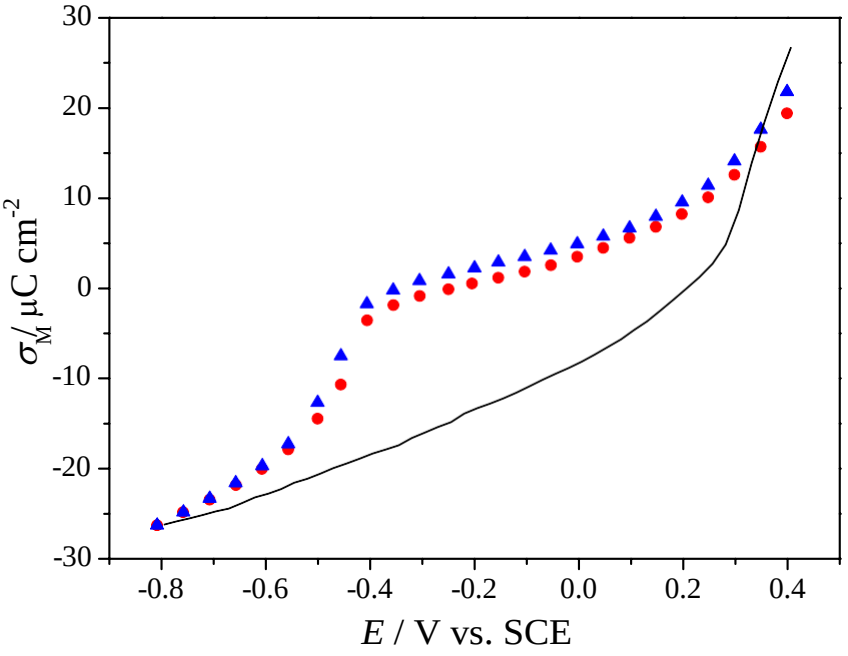

Figure 3. Charge density curves for the bare gold electrode (black) and gold (111) electrodes covered with 1,2-dipalmitoyl-sn-glycero-3-cytidine monolayer with guanine (red circles) and without guanine (blue triangles) in a 0.1 M NaF electrolyte.

3.3. PM-IRRAS results

3.3.1 Acyl chain region between 3050 – 2800 cm^{-1}.

The IR spectra of the CH stretching region for the nucleolipid transferred in the presence of guanine were qualitatively similar to the spectra recorded in the absence of guanine published in our previous paper.[14] To avoid repetition, these spectra are presented in Figure S3a of the Supporting Information. The broad spectral envelope of the CH-stretching region could be deconvoluted (Figure S3b) into four bands centered at 2852 ± 1 cm^{-1} [$\nu_s(CH_2)$], 2874 ± 1cm^{-1} [$\nu_s(CH_3)$] , 2924 ± 1 cm^{-1} [$\nu_{as}(CH_2)$] and 2959 ± 1 cm^{-1} [$\nu_{as}(CH_3)$] and the shoulders on the two sides of the $\nu_{as}(CH_2)$ band correspond to Fermi resonances of the bending vibrations. Figure S3c shows the difference between the experimental spectrum and the sum of deconvoluted bands. It

is small. The positions and widths of the bands are listed in Table S1 of the Supporting Information and appear to be potential-independent. Table S2 lists positions and widths of the bands of the monolayer transferred from water in the absence of guanine. A brief comparison of the two sets of data reveals that although the band positions do not change; the band widths are narrower in the monolayer transferred in the presence of guanine. This behavior suggests that the acyl chains are somewhat better packed in the monolayer transferred in the presence of guanine. When frequencies of the $\nu_s(CH_2)$ and $\nu_{as}(CH_2)$ are less than 2851 cm^{-1} and 2920 cm^{-1}, respectively, the acyl chains assume an all *trans* conformation.[36,37] The values reported in Tables S1 and S2 are at the borderline of these frequency values suggesting that the acyl chains are predominantly in *trans* conformation.

The integrated intensities of symmetric and asymmetric methylene bands can be used to calculate the average angle between *trans* fragments of the chains and the surface normal with the help of equations Eq. S3 and Eq. S4 in the Supporting Information.[38] The average angles of *trans* fragment of the acyl chains are plotted in Figure 4a for the two 1,2-dipalmitoyl-*sn*-glycero-3-cytidine monolayers. The tilt angle is somewhat higher in the presence of guanine and appears to be potential independent. This behavior is consistent with a larger area per molecule in the monolayer transferred from 0.1 M NaF subphase.

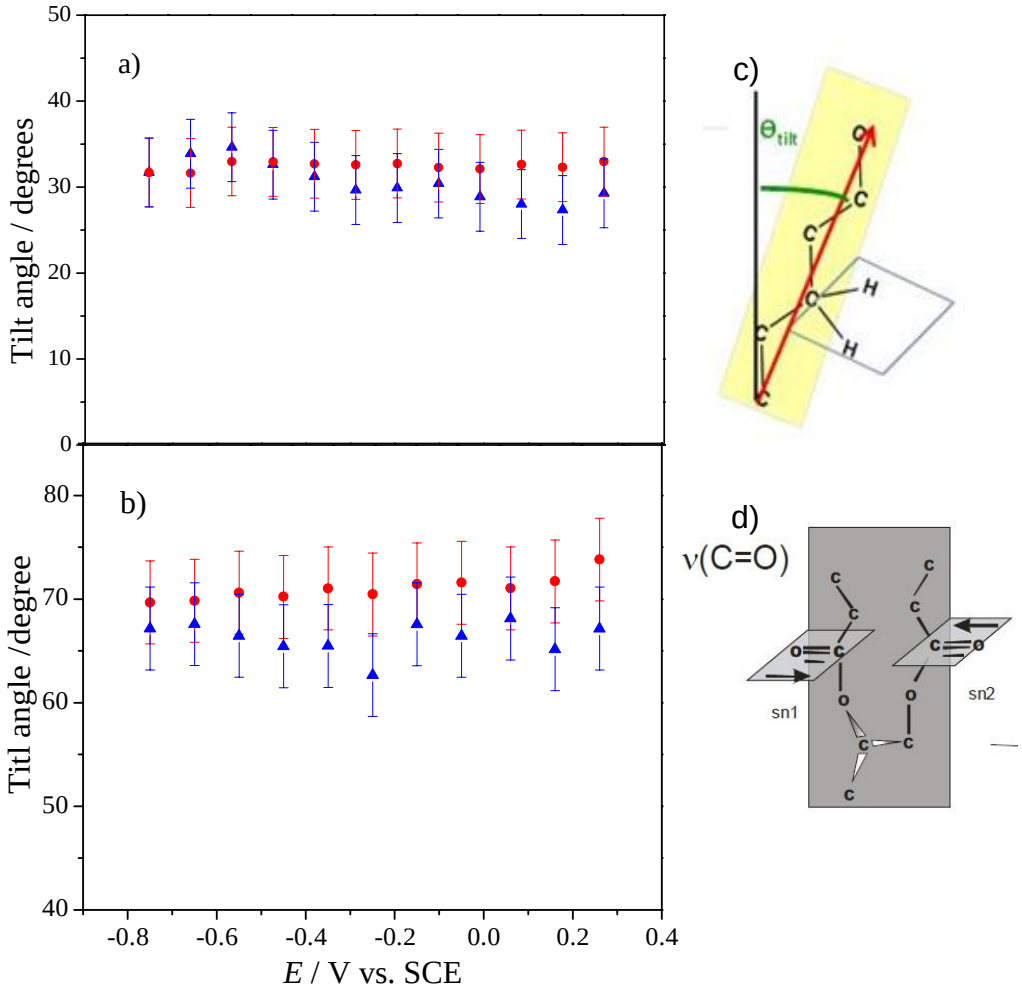

Figure 4. Tilt angle of the a) acyl chains and b) C=O bond of 1,2-dipalmitoyl-sn-glycero-3-cytidine monolayer at gold (111) surface in the presence (red circles) and the absence (blue triangles) of guanine, plotted as a function of the electrode potential. c) and d) are pictorial definition of the tilt angle for the trans fragment of the acyl chains (c) and C=O bond (d).

3.3.2 Polar head region 1800 − 1400 cm^{-1}.

3.3.2.2 IR spectra of the polar head in the presence of guanine

Figure 5a plots the average PM-IRRAS spectrum of 1,2-dipalmitoyl-*sn*-glycero-3-cytidine monolayer in the absence of guanine. For comparison, Figure 5b shows the average spectrum in the presence of guanine. To improve the quality and signal to noise, the PM-IRRAS spectra for the nucleolipids in the absence and presence of guanine were obtained by averaging

all spectra measured for the potentials ranging from −0.75 to 0.36 V vs SCE. The averaged PM-IRRAS spectra show significant differences when guanine is added to the system. The intensities of bands related to C=O (~1730 cm^{-1}) and CH_2 scissoring (~1467 cm^{-1}) modes of acyl chains of the monolayer are lower in the presence of guanine. Figure 4b plots angles between the direction of the transition dipole of the C=O band of the glycerol moiety with respect to surface normal. This transition dipole is oriented along the axis of the C=O bond and hence the tilt angle is a measure of the orientation of the carbonyl group. These angles are somewhat higher in the presence of guanine. Since the chains are more tilted, this behavior suggests that fragments of the chains near the glycerol moiety are somewhat bent upward.

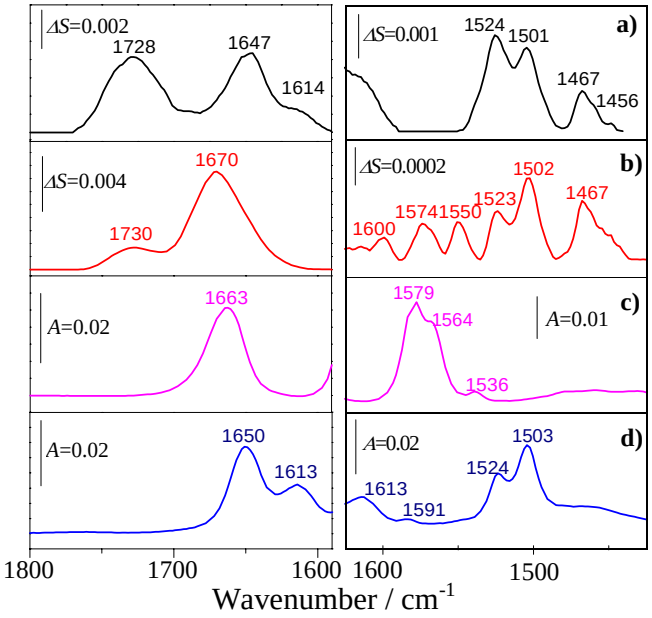

Figure 5. Average PM-IRRAS spectra of 1,2-dipalmitoyl-sn-glycero-3-cytidine monolayer in a) absence and b) presence of guanine. c) Transmission spectrum of the 5 mM guanosine 5-diphosphate in D_2O. d) Transmission spectrum of 5 mM solution of cytidine 5-diphosphate in a 0.1 M NaF/D_2O solution.

The bands in the 1600 - 1500 cm^{-1} region are reduced in the presence of guanine. Figure 5c shows the transmission spectrum of guanosine 5-diphosphate. The bands present in this spectrum correspond to vibrations of the guanine moiety. This spectrum has strong bands at ~1663 and 1579 cm^{-1}. For comparison the transmission spectrum for cytidine 5-diphosphate is

shown in Figure 5d. Overall, Figure 5 shows that spectra corresponding to cytosine and guanosine 5-diphosphates differ significantly from the PM-IRRAS spectrum of 1,2-dipalmitoyl-*sn*-glycero-3-cytidine monolayer in the presence of guanine. This suggests that guanine forms a complex with the cytosine moiety of the nucleolipid.

To assist with IR band assignment, Figure 6 compares two PM-IRRAS spectra measured in the presence of guanine at the most positive potential (i, red curve) and most negative potential (ii, blue curve) to the transmission spectrum of a fully polymeric helix of polyC:polyG complex in D_2O (iii, black curve) taken from literature.[39] Due to different band intensities, separate intensity scales are used for the 1700 – 1625 cm^{-1} region where the C=O stretching bands are located and the 1625 – 1480 cm^{-1} region where the in-plane vibrations of the pyrimidine (C) and purine (G) rings are located.

To assign bands that are associated with the G-C complex, Figure S4 of Supporting Information compares a sum of independently measured transmission spectra of 5 mM solutions of guanosine 5-diphosphate and 5 mM solution of cytidine 5-diphosphate in D_2O, to a transmission spectrum of the (1:1) mixture of 5 mM solutions of guanosine 5-diphosphate and 5 mM solution of cytidine 5-diphosphate in D_2O and to the absorption spectrum of PolyC:PolyG complex in D_2O. The spectra of the sum of independently measured transmission spectra and the mixture of guanosine and cytidine diphosphates are identical indicating that the complex was not formed in the solution. A comparison with the spectrum of the PolyC:PolyG complex shows differences in the 1700-1625 cm^{-1} region where C=O vibrations are located. However, there are very small differences between the three spectra in Figure S4 in the 1600-1500 cm^{-1} region where the ring vibrations are present. With the help of this comparison the bands in the spectrum of PolyC:PolyG complex shown in Figure 6 were assigned to vibrations of guanine (G), cytosine (C) moiety and to the complex (C:G). The two spectral regions will be now discussed separately.

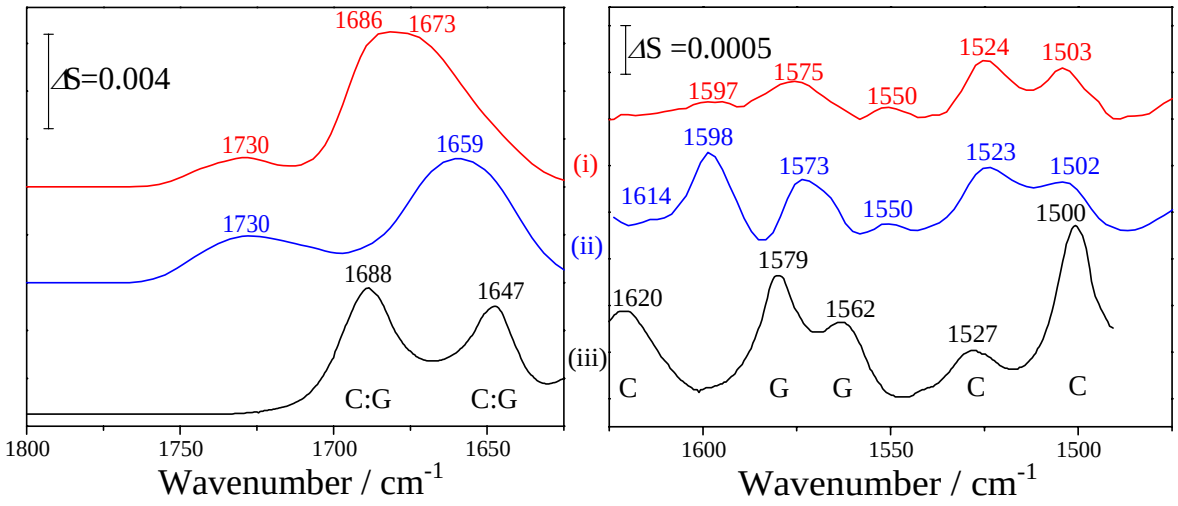

Figure 6 (i) red curve: PM-IRRAS spectrum of 1,2-dipalmitoyl-*sn*-glycero-3-cytidine monolayer at gold (111) surface in the presence of guanine at E = 0.36 V vs SCE; (ii) blue curve: PM-IRRAS spectrum of 1,2-dipalmitoyl-sn-glycero-3-cytidine monolayer on gold (111) surface in the presence of guanine at E=-0.75 V vs SCE; (iii) black curve: absorption spectrum of PolyC:PolyG complex in D_2O taken from Ref.39. The intensity of spectra for PolyC:PolyG complex were adjusted to show bands of intensity comparable to the PM IRRAS spectra.

Figure 7a shows PM-IRRAS spectra in the 1800 – 1625 cm^{-1} region determined for selected electrode potentials. They display a broad envelope of several overlapping bands. The bands between 1750 and 1700 cm^{-1} correspond to C-O stretches of the carbonyl groups of the lipid. The bands of the complex are located in the region between 1700 and 1620 cm^{-1}. Fourier self-deconvolution (FSD) procedure was employed to identify individual bands present in this region. The FSD method narrows the band widths resolving complex spectral features in broad IR envelopes.[40] Figure 7b compares FSD of the PM-IRRAS spectra with the spectrum of the PolyC:PolyG complex taken from ref 39. The spectrum of the complex shows two distinct bands at 1688 and 1647 cm^{-1}. These bands arise from the inter- and intraband coupling between the two C=O stretching vibrations of the cytosine and guanine moieties that are causing an upward shift the 1663 cm^{-1} guanine band by about 20 cm^{-1} and a downward shift of the band of cytosine by about 3 cm^{-1}.[39,41] In the PM-IRRAS spectrum at 0.36 V vs SCE, the presence of

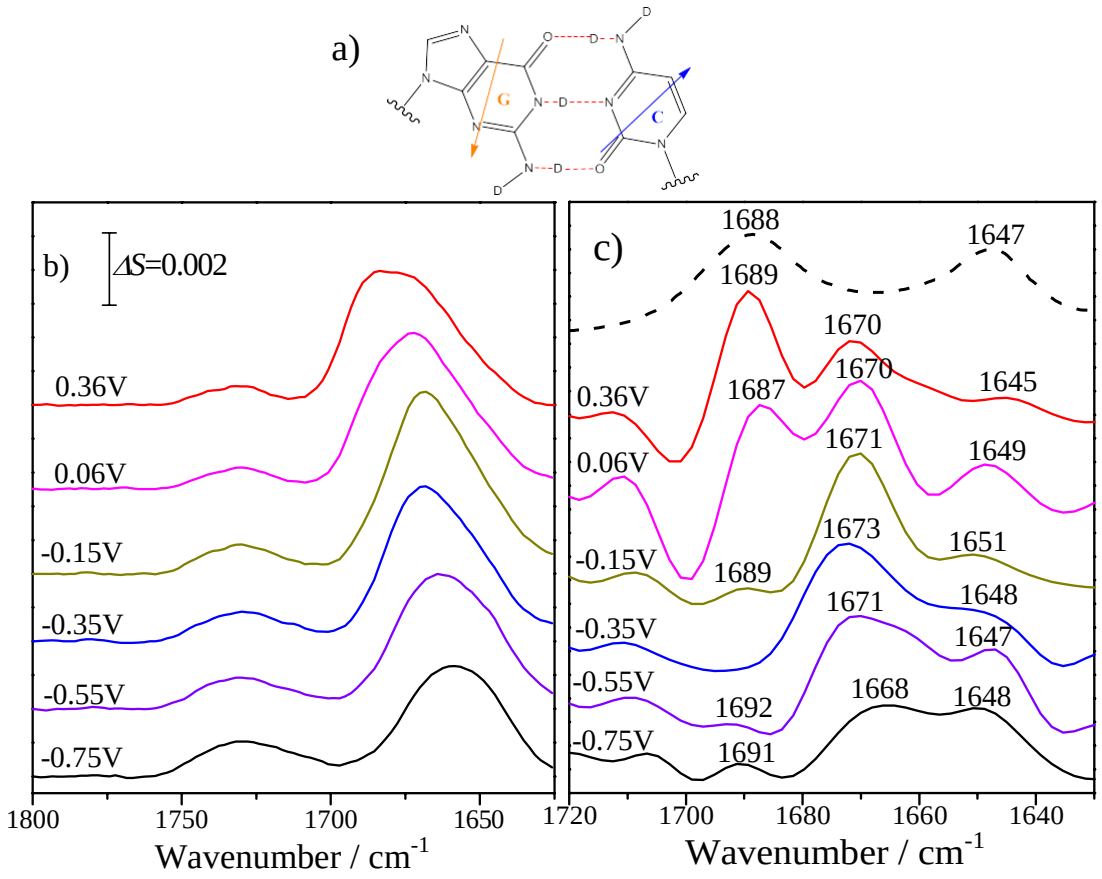

Figure 7. a) Structure of Watson-Crick complex where the arrows show directions of the permanent dipole moments of the guanine and cytosine moieties. b) PM-IRRAS spectra of the 1,2-dipalmitoyl-*sn*-glycero-3-cytidine monolayer at gold (111) surface in presence of guanine in a 0.1 M NaF/D_2O electrolyte at selected electrode potentials. c) FSD of the PM-IRRAS spectra at different potentials (solid lines) and transmission spectrum of PolyC:PolyG complex (dotted line) in D_2O taken from Ref.39. In figure 7c the frequency range was limited to the region that shows bands corresponding to cytosine and guanine.

bands at ~1690 and ~1645 cm^{-1} strongly suggests that the inter and intraband coupling between the C=O vibrations of the two bases is also present in the monolayer, indicating that the Watson-Crick complex was formed.[34,36] However, the presence of ~1670 cm^{-1} band and the broad features of the 1645 cm^{-1} band suggest that a fraction of guanine molecules forms either a weakly coupled bond or their interactions with the nuleolipid have a nonspecific character.

Figure 7b shows that the amplitude of the ~1690 cm^{-1} band becomes reduced and the 1645 cm^{-1} band is shifted to 1648 cm^{-1} when the electrode potential becomes more negative, indicating disappearance of the complex. The strong ~1670 cm^{-1} band suggests that the non-complexed form of guanine is the predominant species in the monolayer. With the help of FSD, the PM-IRRAS spectra were deconvoluted (see Figure S5) and the integrated intensity of the ~1690 cm^{-1} band was calculated. Figure 8 plots the integrated intensity of the ~1690 cm^{-1} band as a function of the electrode potential. For comparison, the charge density on the gold surface (σ_M) is also plotted in Figure 8. Changes of the integrated intensities of the 1690 cm^{-1} band correlate very well with the charge at the gold surface. The correlation shows that the complex is formed when the charge is positive and cytosine moiety in the head region of the monolayer experiences the positive static electric field of the metal. The complex disappears when the charge becomes negative. In conclusion, the present studies demonstrate that guanine binds to the 1,2-dipalmitoyl-*sn*-glycero-3-cytidine monolayer by nonspecific interactions when the interfacial charge is negative and via Watson-Crick complex formation at positive surface charges. In addition, Figure S6 of the Supporting Information plots integrated intensities of the 1690, 1670 and 1648 cm^{-1}bands. For potentials up to -0.35 V vs SCE, the decrease of the intensity of the 1690 cm^{-1} band (corresponding to the complex) correlates well with the increase of the intensity of the 1670 cm^{-1} (non-complexed guanine) and 1648 cm^{-1} band of non-complexed cytosine. This correlation indicates that when potential becomes negative the disappearance of the complex increases surface concentration of non-complexed guanine and cytosine. At potentials more negative than -0.35 V vs SCE the intensities of all three bands decrease. We will show later that this is caused by reorientation of the cytosine and hence most likely guanine molecules. Figure S7 plots ratio of intensities of 1690 to 1670 cm^{-1} bands. This ratio could be used as a rough approximation of the relative amount of the complex. It shows at at the most positive potential its content could be at the order of 35%.

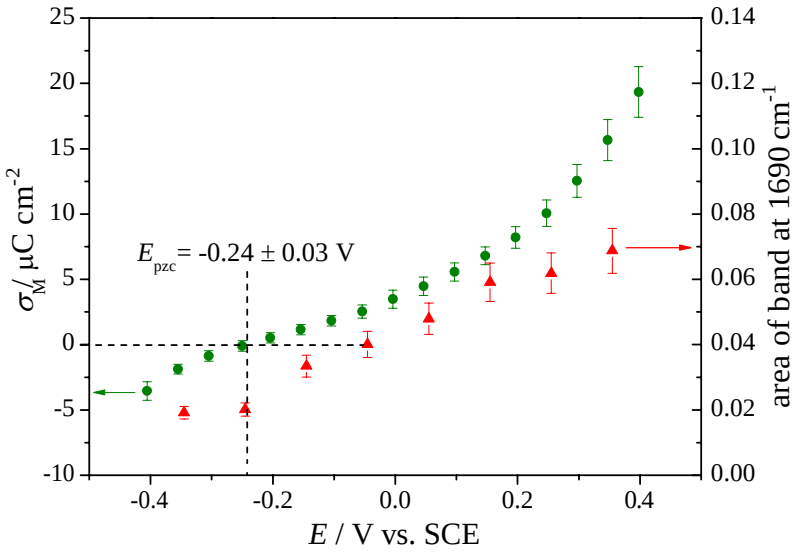

Figure 8. Charge density curve (green circles) and integrated area of the IR band at 1690 cm^{-1} (red triangles).for the gold (111) electrode covered with 1,2-dipalmitoyl-*sn*-glycero-3-cytidine monolayer with guanine in 0.1 M NaF electrolyte as a function of the electrode potential..

The two forms of guanine (the complex and the non-complex forms) were also observed in 1-(2-Octadecyloxycarbonylethyl)cytosine monolayers spread at the air-solution interface of a Langmuir trough, using a D_2O subphase with 1 mM guanosine, and transferred to a CaF_2 substrate.[9] Figure S8 of the Supporting Information compares the spectrum of nine monolayers of 1-(2-Octadecyloxycarbonylethyl)cytosine with bound guanosine[8] to the spectrum of the PolyC:PolyG complex in D_2O.[39] Due to the poor resolution of the digitized spectrum of the multilayers, FSD cannot be applied to resolve the broad 1720 – 1620 cm^{-1} region. The 1691 and 1647 cm^{-1} bands of the complex are present in the broad spectral envelope. However, the band at ~1660 cm^{-1} indicates the presence of a non-complexed guanine moiety (see Figure 5c) suggesting that molecular recognition was also not complete in the experiments described in ref.9.

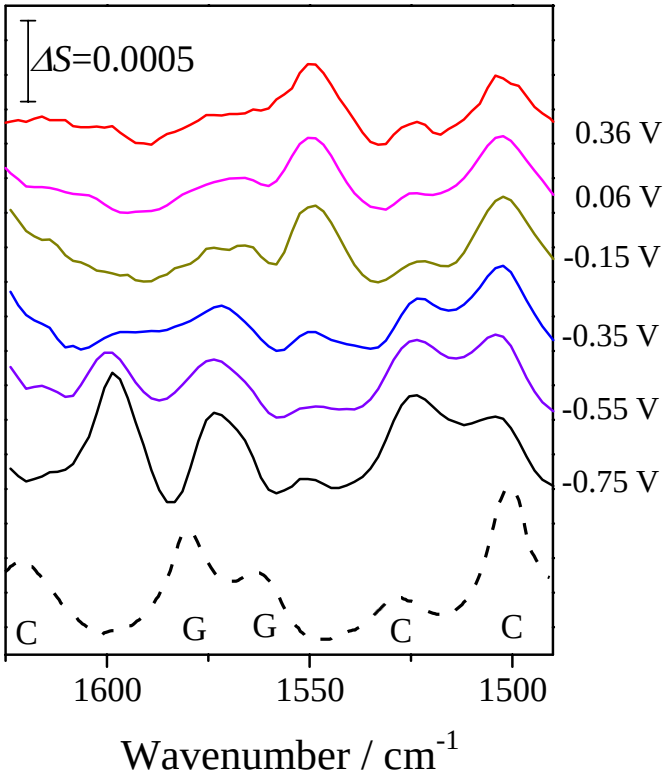

Figure 9. PM-IRRAS spectra of the 1,2-dipalmitoyl-*sn*-glycero-3-cytidine monolayer at gold (111) surface in presence of guanine in the 1625-1490 cm^{-1} region in 0.1 M NaF/D_2O electrolyte at selected electrode potentials. The dashed line represents the absorption spectrum of PolyC:PolyG complex in D_2O taken from Ref.35.

Figure 9 plots PM-IRRAS spectra of the 1625 – 1490 cm^{-1} region recorded for potentials ranging between −0.75 V and 0.36 V vs SCE. These IR vibrations correspond to in-plane vibrations of the of the pyrimidine and purine rings of the two bases. These bands are narrow and well resolved. Figure S5 of the Supporting Information shows their deconvolution. All bands that are present in the PolyC:PolyG complex also are present in the PM-IRRAS spectra. However, PM-IRRAS spectra have two additional bands at ~1600 and ~1550 cm^{-1} that were not present in the spectrum of the complex.

The ~1600 cm^{-1} band was observed in the spectrum of 1-(2-Octadecyloxycarbonylethyl)cytosine with guanosine[9] while the band at ~1550 cm^{-1} was observed for deuterated guanosine samples in KBr.[42] The two bands were assigned to in-plane purine ring vibrations of guanine. Table 1 lists assignment of bands in the PM-IRRAS spectra.

Table 1. Bands observed in the PM-IRRAS spectra of the 1800 – 1500 cm^{-1} region for 1,2-dipalmitoyl-*sn*-glycero-3-cytidine nucleolipid monolayers with guanine the in 0.1 M NaF/D_2O electrolytes.

Wavenumber (cm^{-1})	Assignation of the vibration
1741	$\nu C=O_{(non\text{-}hydrogen\ bonding)}$ ester acyl chain
1728	$\nu C=O_{(hydrogen\ bonding)}$ ester acyl chain
1689	$\nu C=O$ C:G
1670	$\nu C=O$ Guanine
1648	$\nu C=O$ C:G
1598	Cytosine skeletal
1574	Guanine skeletal
1550	Guanine skeletal
1523	$\nu C_4=C_5$ Cytosine
1502	$\nu C_4\text{-}N_7$ Cytosine

Figure 10 plots the results of the two-dimensional correlation spectroscopy (2D COS) analysis.[43,44] The two-dimensional spectroscopy involves calculation of a correlation function between a reference spectrum (average spectrum in this case) and a spectrum recorded at a given potential *E*. It spreads spectral information onto second dimension and hence it assists in revealing presence of bands hidden in a broad spectral envelope of overlapping bands. It has two solutions giving synchronous and asynchronous correlations. [43,44] Figure 10a shows the synchronous spectra and Figure 10b asynchronous spectra. The

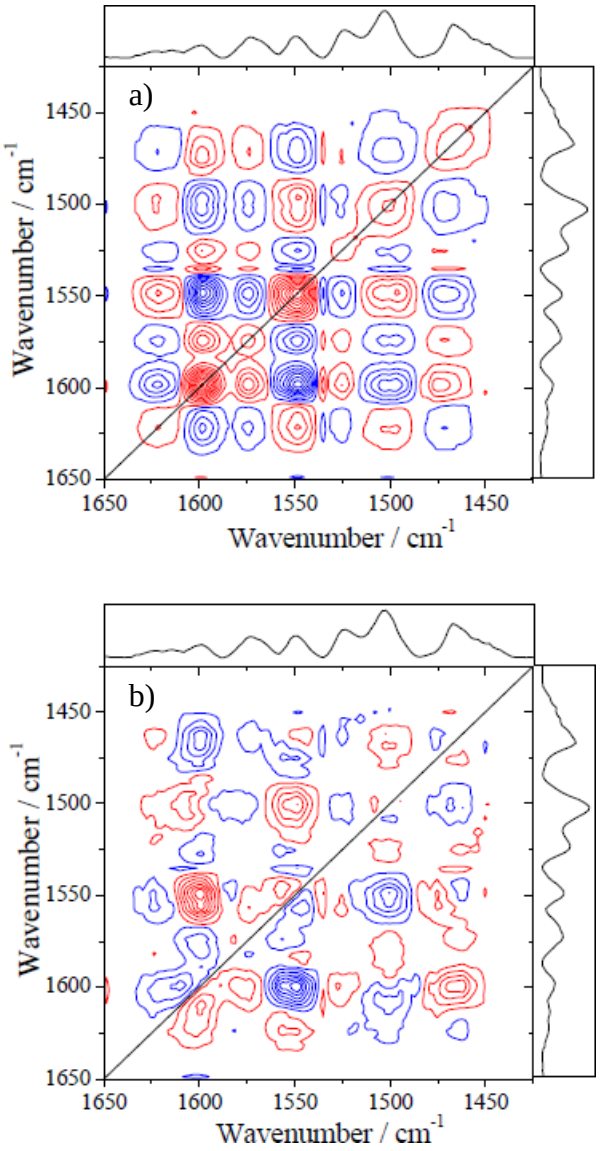

Figure 10. (a) Synchronous and (b) asynchronous 2D COS results of the PM-IRRAS spectra for the 1650 and 1420 cm^{-1} region of the 1,2-dipalmitoyl-*sn*-glycero-3-cytidine monolayer at gold (111) surface in presence of guanine.

Table 2. Signs of bands in the synchronous and asynchronous 2D COS analysis presented in Figure 9.

	1598 C		1574 G		1550 G		1523 C		1502 C	
	asyn	asyn	syn	asyn	syn	asyn	syn	asyn	syn	asyn
1598 C			+	-	-	+	+	-	-	+
1574 G	+	+			-	+	+		-	-
1550 G	-	-	-	-			-	-	+	+
1523 C	+	+	+		-	+			-	-
1502 C	-	+	-	+	+	+	-	+		

blue color shows negative bands and red color positive bands. In synchronous spectrum, the autocorrelation bands are always positive. The positive sign of cross correlation bands indicates that they are changing in the same direction and negative sign indicates that they are changing in the opposite direction. The asynchronous analysis provides information about sequential changes in the PM-IRRAS spectra and consists of no autocorrelation peaks.

The positive sign of a band in asynchronous spectrum indicates that a change at a lower wavenumber takes place before a change at a higher wavenumber. The negative sign indicates that a change at a higher wavenumber takes place before a change at a lower wave number.[44] Table 2 lists signs of bands identified in the 1625 – 1500 cm^{-1} region. This information will now be used to discuss the observed changes in terms of potential induced reorientation and rotation of cytosine and guanine moieties.

3.3.2.3 Potential controlled changes in the orientation and rotation of cytosine and guanine moieties

Table 2 shows that the sign of the (1502C,1523C) band of cytosine moiety is negative in the synchronous spectrum and negative in the asynchronous spectrum. These signs indicate that changes of the two bands are taking place in the opposite direction and that the change at 1523 cm^{-1} occurs before the change at 1502 cm^{-1} band. To gain further information, the intensities of the two bands were integrated and the angle θ between directions of their transition dipoles and surface normal were calculated using Equation S3 of Supporting Information and have been plotted in Figure 11a. The values of θ are 5^o to 10^o higher than in the case of the monolayer without guanine indicating that the cytosine moiety is oriented more parallel to the surface in the presence of guanine. Further, the changes of the tilt angles with potential are small for the 1502 cm^{-1} band. In contrast, the tilt angle of the 1523 cm^{-1} band changes by about 10^o.

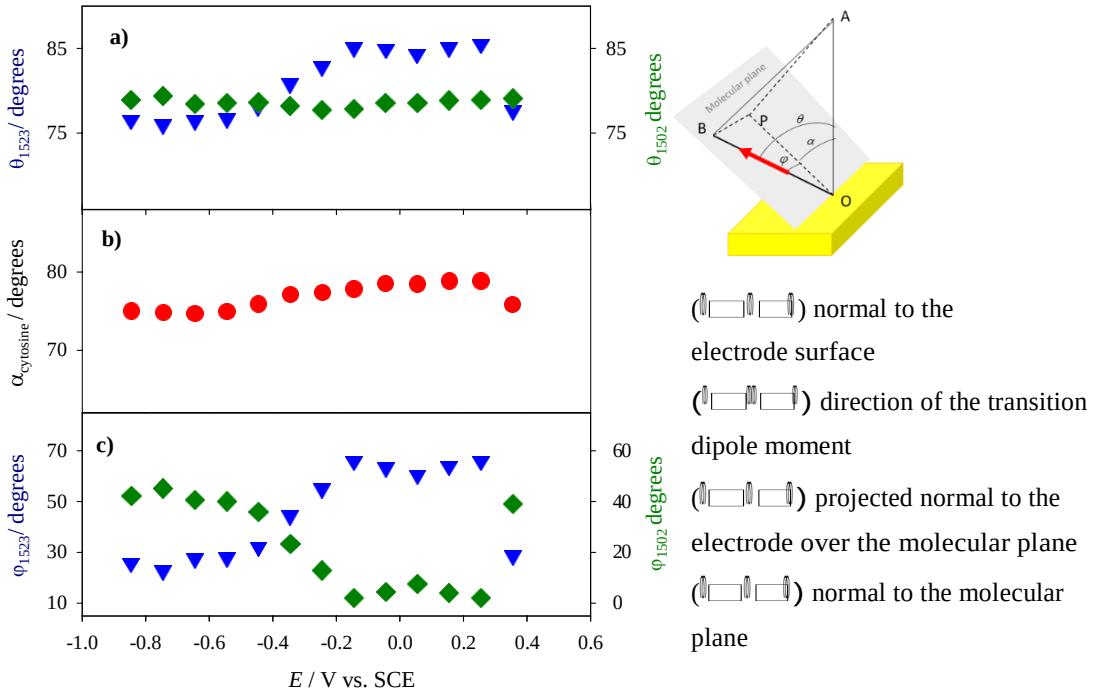

Figure 11. a) Tilt angles of the transition dipole directions of the vibrations at 1502 and 1523 cm^{-1} relative to the normal direction to the electrode. b) Tilt angle of the cytosine moiety plane relative to the normal direction to the electrode surface. c) Angles between the transition dipoles directions of the vibrations at 1502 and 1523 cm^{-1} and the projected normal to the electrode over the cytosine moiety plane. To avoid overcrowding error bars are not shown, however an uncertainty of ± 3° should be applied to every point in this figure. The uncertainties were determined using the procedure described in[45]

The changes of the angle θ could be further decomposed into contributions from the tilt angle of the molecular plane relative to the surface normal (α) and the angle between the transition dipole and the projection of the surface normal on the molecular plane (φ).[1,14] The angle α provides information about the tilt of the plane and the angle φ provides information about rotation of the molecular plane of the cytosine moiety. The definition of angles θ, α and φ is schematically described on the right side of Figure 11. The angles θ, α and φ are related by:[1,14]

$$\cos(\square) = \cos(\square) \times \cos(\square) \qquad (3)$$

DFT calculations were performed to determine the directions of the two transition dipoles in the molecular plane. Using DFT to determine the difference between the angles φ of two in plane

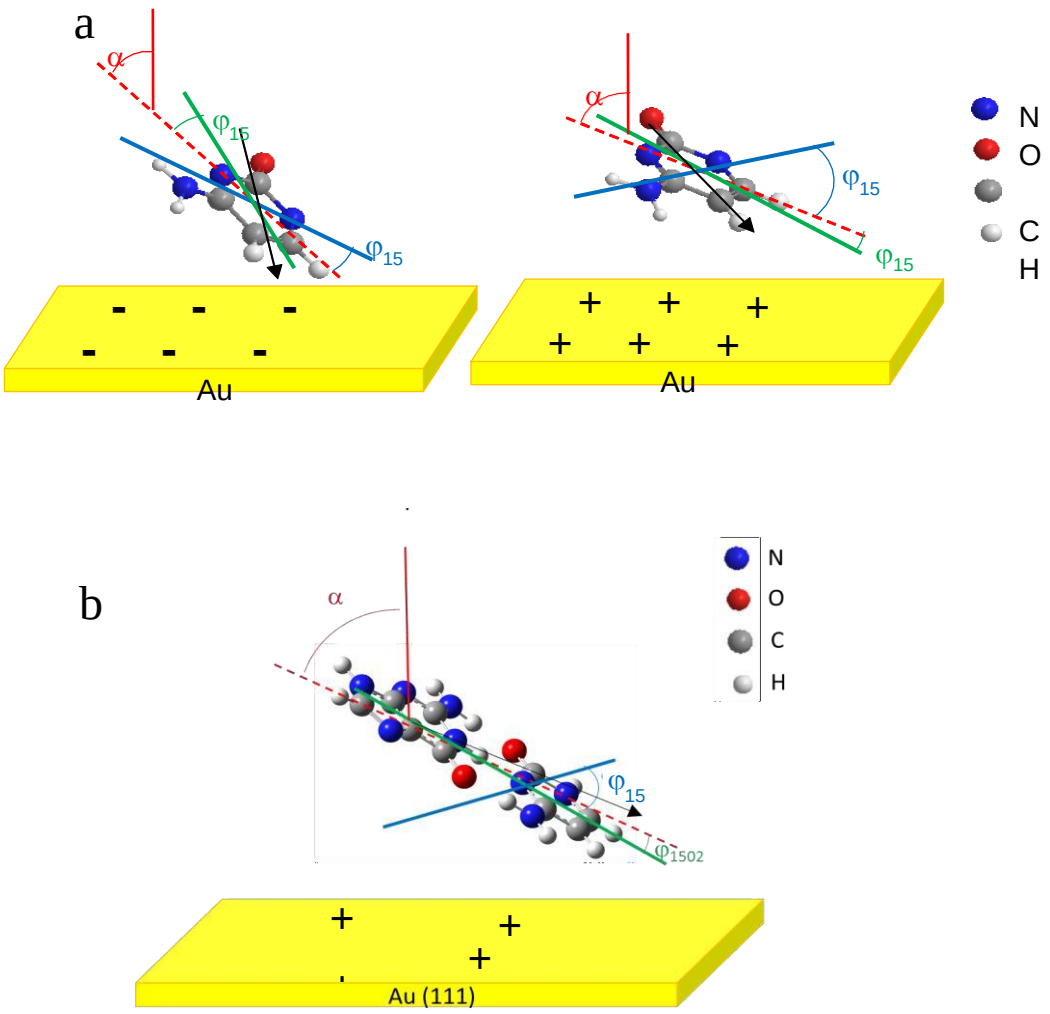

Figure 12. a) Schematic representation of the electric field driven changes in the tilt and rotation of the plane of cytosine moiety in the 1,2-dipalmitoyl-*sn*-glycero-3-cytidine monolayer in the presence of guanine; b) schematic diagram of the orientation of the Watson-Crick complex formed between guanine and cytosine moiety at the 1,2-dipalmitoyl-*sn*-glycero-3-cytidine monolayer surface. The black arrow indicates direction of the permanent dipole moment drown from negative to positive end, green and blue lines plot directions of transition dipole moments of the 1502 and 1523 cm^{-1} bands. Dashed red line marks projection of the surface normal on the plane of cytosine moiety. Symbols + and – indicate sign of the charge on the gold surface generating static electric field in the direction normal to the surface.

vibrations ($|\varphi_1-\varphi_2|$) and knowing angles θ_1 and θ_2, the tilt angle of the molecular plane relative to the surface normal (α) and the angles φ_1 and φ_2 can be determined.[1,14] They are plotted in Figures 11b and c, respectively. The changes of the tilt of the molecular plane are small (~5°).

However, there is a significant rotation of the molecular plane. The changes of angles φ_{1502} and φ_{1523} are on the order of ~40^{o} and taking place at potential ~ −0.28 V vs SCE. This behavior suggests that the changes are driven by the static electric field. Figure 12a shows cartoons illustrating orientation of the cytosine moiety with respect to the electrode surface at positive and negative electric fields. Guidelli and coworkers developed an electrostatic model to calculate the strength of the electric field acting at the head group of a phospholipid monolayer.[46] However, one needs to know thickness and dielectric constant of the polar head region to use this model. These quantities are unknown and their estimate is a subject of a large uncertainty. For this reason we discuss the effect of the static electric field in terms of the field generated by the charge on the metal.

The 2D COS analysis indicated that the change at 1523 cm^{-1} band precedes the change of the 1502 cm^{-1} band. Figure 12a shows that direction of the transition dipole of the 1502 cm^{-1} band is close to the direction of the permanent dipole. Hence, a change in the direction of the permanent dipole is paralleled by a change in the direction of the transition dipole of the 1502 cm^{-1} band. The sequential change of the two bands, therefore, is consistent with the mechanism of the field-permanent dipole driven changes in the orientation and rotation of the plane of cytosine moiety.

Figure 12b shows cartoon of the orientation of the Watson-Crick complex formed at positive potentials. The cartoon was made assuming a planar geometry of the complex and that its orientation is determined by the orientation of cytosine moiety. In this structure, the complex is nearly parallel to the plane of the monolayer surface (it is tilted at an angle ~10^{o}). This orientation optimizes the interactions of the guanine moiety with the nucleolipid monolayer. The nearly parallel orientation is assisted by the interaction of the permanent dipole of the complex with the static electric field. The positive field repels the positive pole of the dipole favoring nearly flat orientation. Negative field is attracting the positive pole of the complex

towards the electrode surface increasing the tilt of the molecule and pushing the guanine molecule towards the solution.

Unfortunately, the exact concentration of guanine molecules within the monolayer is not known. In addition, two forms of guanine molecules are present in the film of the nucleolipid. It is difficult to perform quantitative calculations of the changes in the orientation of the guanine molecule. Therefore, the orientation of guanine in the complex was deduced from the orientation of cytosine moiety. Figure 13a plots the integrated intensities of three bands assigned to guanine moiety, which display significant changes with potential. The onset of these changes coincides with the potential of zero total charge (E_{pztc}) determined to be -0.24 ± 0.04 V vs SCE. The 2D COS analysis shows that for (1502C, 1598C) and (1502C, 1570G) bands, the synchronous peaks are negative and asynchronous peaks are positive. This behavior indicates that the changes take place in the opposite direction and that the change of the 1502 cm^{-1} band of cytosine takes place before the change of the two bands of guanine. Additionally, the (1502C,

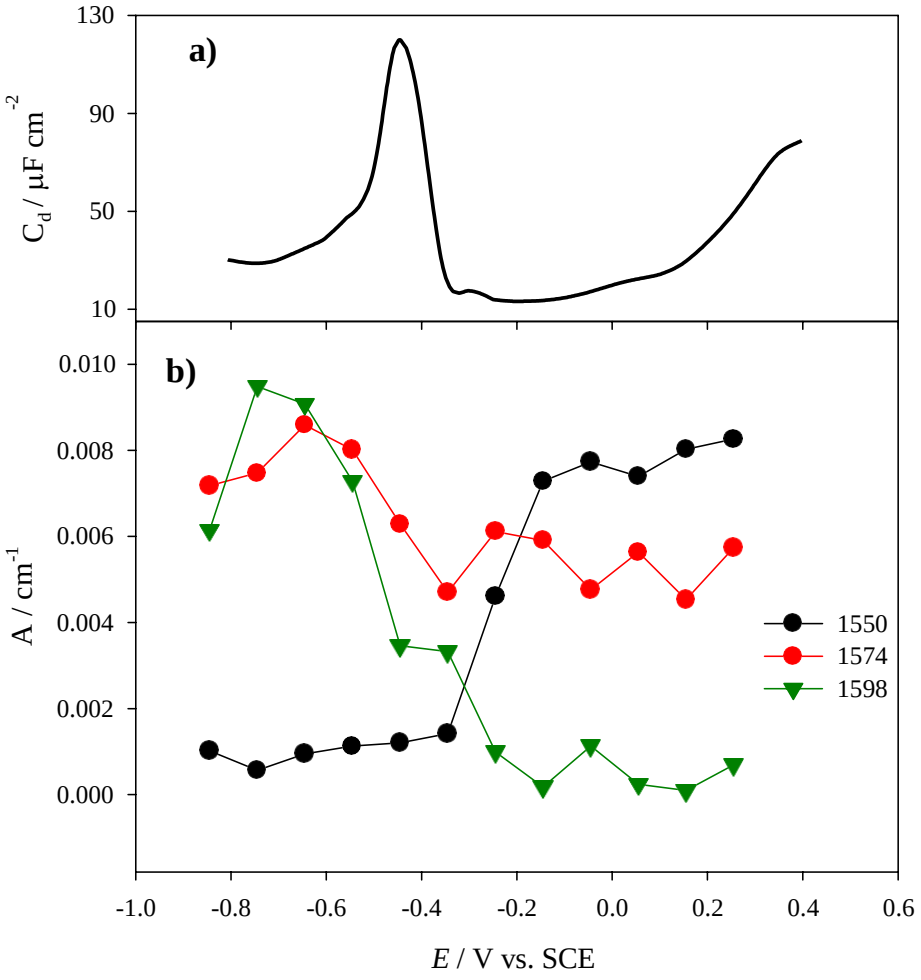

Figure 13 - a) Plot of differential capacitance versus electrode potential obtained by differentiation of the charge density plot in figure 3 for a monolayer of the 1,2-dipalmitoyl-*sn*-glycero-3-cytidine monolayer at gold (111) electrode formed in the presence of guanine. b) Plot of integrated intensities of bands corresponding in plane vibrations of guanine in the 1,2-dipalmitoyl-*sn*-glycero-3-cytidine monolayer at gold (111) electrode as a function of applied potential.

1550G) band is positive in synchronous and negative in asynchronous spectrum. This suggests that the intensities of the two bands change in the same direction and that the change at the 1550 cm^{-1} band take place before the change of the 1502 cm^{-1} band. The intensities of the 1598 and 1574 cm^{-1} bands are small while intensity of the 1550 cm^{-1} band is large when the Watson-Crick complex is formed at positive potentials. Figure 13b plots the differential capacitance curve calculated by differentiation of the charge density curve for a monolayer of the 1,2-dipalmitoyl-

sn-glycero-3-cytidine monolayer at gold (111) electrode formed in the presence of guanine. The comparison of the two data sets indicates that changes of the intensity of the 1598 and 1574 cm^{-1} bands coincide with the onset of the monolayer detachment (desorption) from the electrode surface. In contrast, changes of the intensity of the 1550 cm^{-1} band are completed before the onset of detachment (desorption) of the monolayer. The different behaviors of these bands in the 2D COS spectrum suggest that the 1598 and 1574 cm^{-1} may be assigned to the non-specifically bonded guanine and the 1550 cm^{-1} peak corresponds to the complexed guanine.

4. Conclusions.

The present study demonstrated that the static electric field has a significant effect on the molecular recognition reaction taking place at the metal solution interface. The orientation of the cytosine moiety of the monolayer of 1,2-dipalmitoyl-*sn*-glycero-3-cytidine at the gold (111) electrode surface was controlled by the static electric field of the interface. The orientation of the cytosine moiety influenced the interaction with guanine, its complementary base. When a positive electric field is acting on the molecules, they assume a nearly parallel orientation with respect to the monolayer surface (tilt angle ~10^o). This orientation favors Watson-Crick complex formation. Negative static electric field causes an increase of the tilt of the cytosine moiety to about (15^o – 20^o), which destabilizes the complex and favors non-complex interactions between guanine and the cytidine nucleolipid monolayer.

5. Acknowledgements

The FP and MR acknowledge research grants from Spanish Ministry of Economy and Competitiveness (CTQ2014-57515-C2-1-R) and Andalusian government (PAI-FQM202). JL acknowledges support of the Discovery grant from Natural Sciences and Engineering Council of Canada RG-03958. JAM acknowledges a FPU grant and a Visiting Academic grant from the Spanish Ministry of Science and Technology.

6. Bibliography.

(1) Prieto, F.; Su, Z.; Leitch, J. J.; Rueda, M.; Lipkowski, J. Quantitative Subtractively Normalized Interfacial Fourier Transform Infrared Reflection Spectroscopy Study of the Adsorption of Adenine on Au(111) Electrodes. *Langmuir* **2016**, *32*, 3827–3835.

(2) Prieto, F.; Alvarez-Malmagro, J.; Rueda, M. Electrochemical Impedance Spectroscopy Study of the Adsorption of Adenine on Au(111) Electrodes as a Function of the pH. *J. Electroanal. Chem.* **2017**, *793*, 209–217.

(3) Alvarez-Malmagro, J.; Rueda, M.; Prieto, F. In Situ Surface-Enhanced Infrared Spectroscopy Study of Adenine-Thymine Co-Adsorption on Gold Electrodes as a Function of the pH. *J. Electroanal. Chem.* **2018**, *819*, 417–427.

(4) Alvarez-Malmagro, J.; Prieto, F.; Rueda, M.; Rodes, A. In Situ Fourier Transform Infrared Reflection Absortion Spectroscopy Study of Adenine Adsorption on Gold Electrodes in Basic Media. *Electrochim. Acta* **2014**, *140*, 476–481.

(5) Rueda, M.; Prieto, F.; Álvarez-Malmagro, J.; Rodes, A. Evidences of Adenine-Thymine Interactions at Gold Electrodes Interfaces as Provided by in-Situ Infrared Spectroscopy. *Electrochem. Commun.* **2013**, *35*, 53–56.

(6) Prieto, F.; Alvarez-Malmagro, J.; Rueda, M.; Orts, J. M. Tautomerism of Adsorbed Thymine on Gold Electrodes: An in Situ Surface-Enhanced Infrared Spectroscopy Study. *Electrochim. Acta* **2016**, *201*, 300–310.

(7) Čoga, L.; Masiero, S.; Drevenšek-Olenik, I., Lamellar versus compact self-assembly of lipoguanosine derivativesin thin surface films, *Colloids and Surfaces B: Biointerfaces* **2014**, *121*,114–121.

(8) Wang, Y.; Du, X.; Miao, W.; Liang, Y. Molecular Recognition of Cytosine- and Guanine-Functionalized Nucleolipids in the Mixed Monolayers at the Air - Water Interface and Langmuir - Blodgett Films. *J. Phys. Chem. B* **2006**, *110(10)*, 4914–4923.

(9) Miao, W.; Du, X.; Liang, Y. Molecular Recognition of Nucleolipid Monolayers of 1-(2-Octadecyloxycarbonylethyl) Cytosine to Guanosine at the Air-Water Interface and Langmuir - Blodgett Films. *Langmuir* **2003**, 19, 5389–5396.

(10) Miao, W.; Luo, X.; Liang, Y. Molecular Recognition of 7-(2-Octadecyloxycarbonylethyl)-Guanine to Cytidine at the Air/Water Interface and LB Film Studied by Fourier Transform Infrared Spectroscopy. *Spectrochim. Acta Part A: Mol.*

and Biomol. Spectrosc. **2003**, *59*, 1045–1050.

(11) Miao, W.; Luo, X.; Wu, S.; Liang, Y. Fourier Transform Infrared Spectroscopy Study on Order-Disorder Transition in Langmuir-Blodgett Films of 7-(2-Octadecyloxycarbonylethyl)-Guanine before and after Recognition to Cytidine. *Spectrochim. Acta Part A: Mol. and Biomol. Spectrosc.* **2004**, *60*, 413–416.

(12) Čoga, L.; Spindler, L.; Masiero, S.; Drevenšek-Olenik, I. Molecular Recognition of a Lipophilic Guanosine Derivative in Langmuir Films at the Air-Water Interface. *Biochim. Biophys.Acta - Gen. Subj.* **2017**, *1861*, 1463–1470.

(13) Huang, J.; Li, C.; Liang, Y. FT-SERS Studies on Molecular Recognition Capabilities of Monolayers of Novel Nucleolipid Amphiphiles. *Langmuir* **2000**, *16* (8), 3937–3940.

(14) Alvarez-Malmagro, J.; Su, Z.; Leitch, J. J.; Prieto, F.; Rueda, M.; Lipkowski, J. Spectroelectrochemical Characterization of 1,2-Dipalmitoyl-Sn-Glycero-3-Cytidine Diphosphate Nucleolipid Monolayer Supported on Gold (111) Electrode. *Langmuir* **2019**, *35*, 901–910.

(15) Watson, J. D. & Crick, F. H. C. Molecular Structure of Nucleic Acids. *Nature* **1953**, *171*, 737–738.

(16) Richer, J.; Lipkowski, J. Measurement of Physical Adsorption of Neutral Organic-Species at Solid Electrodes. *J. Electrochem. Soc.* **1986**, *133* (1), 121–128.

(17) Stolberg, L.; Morin, S.; Lipkowski, J.; Irish, D. E. Adsorption of Pyridine at the Gold (111) -Solution Interface. *J. ELectroanal Chem.* **1991**, *307* (111), 241–262.

(18) Kunze, J.; Leitch, J.; Schwan, A. L.; Faragher, R. J.; Naumann, R.; Schiller, S.; Knoll, W.; Dutcher, J. R.; Lipkowski, J.; Planck, M. New Method to Measure Packing Densities of Self-Assembled Thiolipid Monolayers. *Langmuir* **2006**, *22* (23), 5509–5519.

(19) Laredo, T.; Leitch, J.; Chen, M.; Burgess, I. J.; Dutcher, J. R. Measurement of the charge number per adsorbed molecule and packing densities of self-assembled long-chain monolayers of thiols. *Langmuir* **2007**, *23*, 6205–6211.

(20) Li, N.; Zamlynny, V.; Lipkowski, J.; Henglein, F.; Pettinger, B. In Situ IR reflectance Absorption Spectroscopy Studies of Pyridine Adsorption at the Au(110) Electrode Surface. *J. Electroanal. Chem.* **2002**, *524–525*, 43–53.

(21) Zamlynny, V.;Lipkowski, J. *Quantiative SNIFTIRS and PM IRRAS of Organic Molecules at Electrode Surfaces.,* Advances in Electrochemistry and Electrochemical

Engineering; R.Alkire, D.M.Kolb, J. L. and P. N. R. (Eds), Ed.; Vol. 9, **2006**, pp 315-376.

(22) Nagle, J. F.; Tristram-Nagle, S. Structure of Lipid Bilayers. *Biochim. Biophys. Acta* **2000**, *1469*, 159–195.

(23) Palik, E. Handbook of Optical Constants of Solids II, Academic Press; San Diego, **1998**.

(24) Bertie, J.E.; Ahmed, M.K.; Eysel, H.H.; Infrared intensities of liquids. 5. Optical and dielectric constants, integrated intensities, and dipole moment derivatives of H_2O and D_2O at 22 degree, *J. Phys. Chem*., **1989**,93,2210-2218.

(25) Perdew, J. P.; Ernzerhof, M.; Burke, K.; Perdew, J. P.; Ernzerhof, M.; Burke, K. Rationale for Mixing Exact Exchange with Density Functional Approximations. *J. Chem. Phys.*. **1996**, 105 (22), *9982*-9985.

(26) Scuseria,E.; Robb, M. A.; Cheeseman, J. R.; Scalmani, G.; Barone, V.; Mennucci, B.; Petersson, G. A.; Nakatsuji, H.; Caricato, M.; Li, X.; Hratchian, H. P.; Izmaylov, A. F.; Bloino, J.; Zheng, G. ; Sonnenberg, J. L.; Hada, M. ; Ehara, M. ; Toyota, K.; Fukuda, R.; Hasegawa, J.; Ishida, M.; Nakajima, T.; Honda, Y.; Kitao, O.; Nakai, H.; Vreven, T.; Montgomery, Jr. J. A.; Peralta, J. E.; Ogliaro, F.; Bearpark, M. ; Heyd, J. J.; Brothers, E.; Kudin, K. N.; Staroverov, V. N.; Kobayashi, R.; Normand, J.; Raghavachari, K.; Rendell, A.; Burant, J. C.; Iyengar, S. S.; Tomasi, J. ; Cossi, M.; Rega, N.; Millam, J. M.; Klene, M. ; Knox, J. E.; Cross, J. B.; Bakken, V. ; Adamo, C. ; Jaramillo, J.; Gomperts, R.; Stratmann, R. E.; Yazyev, O.; Goldstin, A. J.; Cammi, R.; Pomelli, C.; Ochterski, J. W.; Martin, R. L.; Morokuma, K.; Zakrzewski, V. G.; Voth, G. A.; Salvador, P.; Dannenberg, J. J.; Dapprich, S. ; Daniels, A. D.; Farkas, Ö. ; Foresman, J. B.; Ortiz, J. V.; Cioslowski, J.; Fox, D. J. Gaussian 09 (Ggoldssian, Inc., Wallingford CT, 2009).

(27) Alies, B.; Oelhazi,M.A.; Patwa,A.; Verget,J.; Navailles,L.; Desvergues, V.; Barthelemy, P., Cytidine-and guanosine based nucleotide lipids, *Org.Biomol.Chem.* **2018**, 16, 4888-4894.

(28) Miyoshi, T.; Kato, S. Detailed Analysis of the Surface Area and Elasticity in the Saturated 1,2-Diacylphosphatidylcholine / Cholesterol Binary Monolayer System. *Langmuir* **2015**, *31*, 9086–9096.

(29) Lipkowski, J.; Shi, Z., Chen; A., Pettinger, B.; Bilger, C. Ionic Adsorption at the Au(111) Electrode Surface. *Electrochim. Acta.* **1998**, *43* (19–20), 2875–2888.

(30) Seenath, R., Leitch, J. J., Su, Z., Faragher, R. J., Schwan, A. L., & Lipkowski, J. Measurements of surface concentration and charge number per adsorbed molecule for a thiolipid monolayer tethered to the Au (111) surface by a long hydrophilic chain. *J.*

Electroanal. Chem., **2017**, 793, 203-208.

(31) Priske, G., Su, Z., Abbasi, F., Lipkowski, J., & Auzanneau, F. I. Synthesis and electrochemical characterization of 4-thio pseudo-glycolipids as candidate tethers for lipid bilayer models. *Electrochim. Acta*, **2019**, 298, 150-162.

(32) Kunze, J.; Leitch, J.; Schwan, A. L.; Faragher, R. J.; Naumann, R.; Schiller, S.; Knoll, W.; Dutcher, J. R.; Lipkowski, J. New Method to Measure Packing Densities of Self-Assembled Thiolipid Monolayers. *Langmuir* **2006**, *22* (12), 5509–5519

(33) Burgess, I.; Li, M.; Horswell, S. L.; Szymanski, G.; Lipkowski, J.; Majewski, J.; Satija, S. Electric Field-Driven Transformations of a Supported Model Biological Membrane--an Electrochemical and Neutron Reflectivity Study. *Biophysical Journal* **2004**, *86* (3), 1763–1776.

(34) Horswell, S. L.; Zamlynny, V.; Li, H. Q.; Merrill, A. R.; Lipkowski, J. Electrochemical and PM-IRRAS Studies of Potential Controlled Transformations of Phospholipid Layers on Au(111) Electrodes. *Faraday Discuss.***2002**, *121* (1), 405–422

(35) Bizzotto, D.; Zamlynny, V.; Burgess, I.; Jeffrey, C. A.; Li, H. Q.; Rubinstein, J.; Galus, Z.; Nelson, A.; Pettinger, B.; Merrill, A. R.; Lipkowski, J. Amphiphilic and Ionic Surfactants at Electrode Surfaces. In Interfacial Electrochemistry, Theory, Experiment and Applications; Wieckowski, A., Ed.; **1999**; p 405-426

(36) Mantsch, H. H.; McElhaney, R. N. P. Phospholipid Phase Transitions in Model and Biological Membranes as Studied by Infrared Spectroscopy. *Chem. Phys. Lipids* **1991**, *57* (2–3), 213–226

(37) Casal, H. L.; Mantsch, H. H. Polymorphic Phase Behaviour of Phospholipid Membranes Studied by Infrared Spectroscopy. *Biochim. Biophys. Acta* **1984**, *779* (4), 381–401.

(38) Kycia, A.H; Su, Z-F; Brosseau, C. L; Lipkowski, J, In Situ PM-IRRAS Studies of Biomimetic Membranes Supported at Gold Electrode Surfaces in "Vibrational Spectroscopy at Electrified Interfaces." Carol Korzeniewski, Bjoern Braunschweig and Andrzej Wieckowski, (Ed), Wiley-VCH, New York, **2013**; pp 345-417.

(39) Howard, F. B.: Frazier, J.; Miles, H. T., Interbase vibrational coupling in G:C polynucleotide helices. PNAS, **1969**, 64, 451-458.

(40) Surewicz, W.; Mantsch, H. New Insight into Protein Secondary Structure from Resolution-Enhanced Infrared Spectra. *Biochim. Biophys. Acta* **1988**, *952* (2), 115–130.

(41) Krummel, A.T.; Mukherjee, P.; Zanni,M.T.; Inter and intraband vibrational coupling in

DNA studied with heterodyned 2D-IR spectroscopy, *J.Phys.Chem.B*, **2003**,107,9165-9169

(42) Shimanouchi, T.; Tsuboi, M.; Kyogoku, Y. Infrared Spectra of Nucleic Acids and Related Compounds. *Adv.Chem.Phys.* **1965**, *7*, 435–498

(43) Noda, I.; Dowrey, A. E.; Marcott, C.; Story, G. M.; Ozaki, Y, Generalized two-dimensional correlation spectroscopy. *Applied Spectroscopy*, **2000**, 54(7), 236A-248A.

(44) Noda, I. Two-Dimensional Codistribution Spectroscopy to Determine the Sequential Order of Distributed Presence of Species. *J. Mol. Struct.* **2014**, *1069*, 50–59.

(45) Bin, X.; Horswell, S. L.; Lipkowski, J. Electrochemical and PM-IRRAS Studies of the Effect of Cholesterol on the Structure of a DMPC Bilayer Supported at an Au (111) Electrode Surface , Part 2: Properties of the Head Group Region. *J.Phys.Chem.B*, **2006**, 110, 26430-26441

(46) Moncelli, M. R.; Becucci, L.; Buoninsegni, F. T.; Guidelli, R. Surface Dipole Potential at the Interface between Water and Self- Assembled Monolayers of Phosphatidylserine and Phosphatidic Acid. *Biophys. J.* **1998**, *74* (5), 2388–2397.

TOC graphics